Vol. 567: 41–56, 2017
https://doi.org/10.3354/meps12033

MARINE ECOLOGY PROGRESS SERIES
Mar Ecol Prog Ser

Published March 13

Nitrogen nutritional condition affects the response of energy metabolism in diatoms to elevated carbon dioxide

Haizheng Hong[1,2], Dongmei Li[1], Wenfang Lin[1], Weiying Li[1], Dalin Shi[1,2,*]

[1]State Key Laboratory of Marine Environmental Science, Xiamen University, Xiamen, Fujian 361102, PR China
[2]Key Laboratory of the Ministry of Education for Coastal and Wetland Ecosystems, Xiamen University, Xiamen, Fujian 361102, PR China

ABSTRACT: Marine phytoplankton are expected to benefit from enhanced carbon dioxide (CO_2), attributable largely to down-regulation of the CO_2 concentrating mechanism (CCM) which saves energy resources for other cellular processes. However, the nitrogen (N) nutritional condition (N-replete vs. N-limiting) of phytoplankton may affect the responses of their intracellular metabolic processes to elevated CO_2. We cultured the model diatoms *Thalassiosira pseudonana*, *Phaeodactylum tricornutum*, and *Thalassiosira weissflogii* at ambient and elevated CO_2 levels under N-replete and N-limiting conditions. Key metabolic processes, including light harvesting, C fixation, photorespiration, respiration, and N assimilation, were assessed systematically and then incorporated into an energy budget to compare the effects of CO_2 on the metabolic pathways and the consequent changes in photosynthesis and C fixation as a result of energy reallocation under the different N nutritional conditions. Under the N-replete condition, down-regulation of the CCM at high CO_2 was the primary contributor to increased photosynthesis rates of the diatoms. Under N-limiting conditions, elevated CO_2 significantly affected the photosynthetic photon flux and respiration, in addition to CCM down-regulation and declines in photorespiration, resulting in an increase of the C:N ratio in all 3 diatom species. In *T. pseudonana* and *T. weissflogii*, the elevated C:N ratio was driven largely by an increased cellular C quota, whereas in *P. tricornutum* it resulted primarily from a decreased cellular N quota. The N-limited diatoms therefore could fix more C per unit of N in response to elevated CO_2, which could potentially provide a negative feedback to the ongoing increase in atmospheric CO_2.

KEY WORDS: Ocean acidification · N-limitation · Energy budget · C:N ratio · Diatoms

INTRODUCTION

Human activities such as fossil fuel combustion, cement production, and deforestation have caused atmospheric carbon dioxide (CO_2) levels to increase by nearly 40% over the past 250 yr (Feely et al. 2009). If this anthropogenic emission continues unabated, atmospheric CO_2 concentrations will reach 800 µatm by the end of this century (Orr et al. 2005). The oceans have tempered the rapid rise in atmospheric CO_2 by absorbing about a third of the anthropogenic CO_2 released (Sabine et al. 2004, Sabine & Feely 2007). However, the dissolution of anthropogenic CO_2 in the surface ocean leads to substantial perturbations in seawater dissolved inorganic C chemistry. As a result, the concentrations of dissolved CO_2 and bicarbonate (HCO_3^-) increase, whereas seawater pH and the concentration of carbonate (CO_3^{2-}) decrease. Collectively, these chemical changes are commonly referred to as ocean

*Corresponding author: dshi@xmu.edu.cn

acidification (Caldeira & Wickett 2003, Doney et al. 2009).

Diatoms account for ~40% of primary production in the ocean and are assumed to dominate the sequestration of C to the deep ocean (Falkowski et al. 2004). Diatoms possess efficient CO_2 concentrating mechanisms (CCMs), which elevate the CO_2 concentration at the site of C fixation by the enzyme RuBisCO (Reinfelder 2011). However, the CCM is an energy-expensive and nutrient-intensive process, requiring ~1.5 to 6 ATPs for C transport per C fixed and thereby raising the energy cost of C fixation by 13 to 51%, in addition to the minimum energy required to fix C via the Calvin cycle (Hopkinson et al. 2011). It has been suggested that elevated partial pressure of CO_2 (pCO_2) in seawater as a result of ocean acidification will down-regulate the CCM to reduce demands for resources and energy and thus can help stimulate primary production (Tortell et al. 2008, Hopkinson et al. 2011).

A higher rate of photosynthetic C fixation or growth at elevated CO_2 is observed in some, although not all, nutrient-replete laboratory cultures of diatoms (e.g. Wu et al. 2010, Yang & Gao 2012). However, primary production is limited by nitrogen (N) in vast regions of the ocean (Moore et al. 2013). Moreover, sea surface warming caused by rising atmospheric CO_2 will augment water column stratification, thereby intensifying N limitation as a result of the reduced nutrient supply from deep waters (Doney 2006). Even in coastal areas or upwelling zones, where N is generally not a limiting factor, phytoplankton can still experience depletion of the N source soon after the initiation of a bloom (Taucher et al. 2015). In contrast to N-replete cultures, increased CO_2 reduces the photosynthetic rate of the diatom *Thalassiosira pseudonana* grown under N-limiting conditions, despite the fact that the CCM is down-regulated (Hennon et al. 2014). Additionally, the expression levels of photosynthetic, photorespiratory, and respiratory genes in *T. pseudonana* are also reduced under N limitation, suggesting a reduction in general metabolism in N-limited diatoms at high CO_2 (Hennon et al. 2015).

The particulate C:N ratio is one of the most influential factors affecting the strength of the marine biological pump (Broecker 1982), and its change in response to elevated CO_2 varies substantially among different species of phytoplankton under N-replete conditions (Burkhardt et al. 1999, Reinfelder 2012). This may be due to subtle changes or to species-specific differences in response to the changing environment. On the other hand, it has been demonstrated in a few studies that in an N-limited and diatom-dominated phytoplankton community, the C:N ratio or the uptake ratio of dissolved inorganic C over nitrate (NO_3^-) increases at high CO_2 (Riebesell et al. 2007, Losh et al. 2012).

Table 1. Enzymes involved in key metabolic processes and the regulatory levels at which they were quantitatively assessed

Metabolic processes	Enzymes	Regulatory levels assessed
C fixation	PsbA	Protein expression
	PsaC	Protein expression
	RbcL	Protein expression
	CA	Gene transcription
Photorespiration	PGP	Gene transcription
	GDCT	Gene transcription
Respiration	COX1	Gene transcription
N assimilation	NR	Protein expression
		Enzymatic activity

These studies suggest that phytoplankton metabolism responds differently to increased CO_2 under N-replete versus N-limiting conditions (Burkhardt et al. 1999, Losh et al. 2012, Reinfelder 2012). In the present study, we cultured the model diatoms *T. pseudonana*, *Phaeodactylum tricornutum*, and *T. weissflogii* under both N-replete and N-limiting conditions. Key metabolic processes, including light harvesting, C fixation, photorespiration, respiration and N assimilation, were quantitatively assessed (Table 1), and then incorporated into an energy budget to compare the effects of elevated pCO_2 on the cellular metabolic pathways and the consequent changes in photosynthesis and C fixation as a result of energy reallocation under the different N nutritional conditions (Shi et al. 2015). We believe this direct comparison between the different N conditions will provide insights into the mechanisms underlying the responses of diatoms to rising atmospheric CO_2 and will advance our understanding of how these responses may potentially affect the C biogeochemical cycle in the future ocean.

MATERIALS AND METHODS

Cell culturing and experimental design

Axenic cultures of the diatoms *Thalassiosira pseudonana* (Strain no. CCMP 1335), *Phaeodactylum*

tricornutum (CCMP 630), and *T. weissflogii* (CCMP 1336) were obtained from the Provasoli-Guillard National Center for Marine Algae and Microbiota (Maine, USA). Sterile techniques were applied for culturing and experimental manipulations. The diatoms were grown in 0.22 µm-filtered and microwave-sterilized oligotrophic surface seawater from the South China Sea, which was amended with Aquil* concentrations of nutrients (Sunda et al. 2005). All chemicals used were purchased from Sigma-Aldrich Chemical. The cultures were maintained in the exponential phase and grown semi-continuously at 20°C under continuous light (150 µmol photons m^{-2} s^{-1}) in an AL-41L4 algal chamber (Percival). Cells were pre-acclimated at 2 CO_2 levels (i.e. 400 and 750 µatm), achieved by gentle bubbling with humidified and 0.22 µm-filtered CO_2-air mixtures, which were delivered using CO_2 mixers (Ruihua Instrument & Equipment).

After pre-acclimation for approximately 50 generations, triplicate batch cultures of the diatoms were then grown in 1 l sterilized polycarbonate bottles (Nalgene Labware) for at least 10 generations. Cells in mid-exponential phase were harvested for analysis as N-replete treatments. For N-limited treatments, another triplicate batch of cultures of diatom cells were grown in Aquil* media except that 15 µM (instead of 100 µM) of NO_3^- was used. The cultures were harvested at 36 h and 72 h after entering the stationary phase, which were designated as N limited-1 and N limited-2, respectively (Fig. A1 in Appendix 1). Cell numbers were counted daily using a Z2 Coulter Counter (Beckman Coulter). The specific growth rates were determined from linear regressions of the natural logarithm of cell number versus time.

Table 2. Carbonate chemistry in cultures of the diatoms *Thalassiosira pseudonana*, *Phaeodactylum tricornutum*, and *T. weissflogii* acclimated to 2 different pCO_2 levels (400 and 750 µatm) under different N nutritional conditions (N nutri. cond.). N limited-1 and N limited-2 represent cultures harvested at 36 and 72 h after entering the stationary phase, respectively (Fig. A1 in Appendix 1). Alkalinity and pCO_2 were calculated from pH_T, dissolved inorganic carbon (DIC), temperature, salinity, PO_4^{3-} and SiO_4^{2-} using the CO2Sys program (Pierrot et al. 2006) with equilibrium constants K_1 and K_2 in Mehrbach et al. (1973) refitted by Dickson & Millero (1987). Data are mean ± SD (n = 3)

Diatom N nutri. cond.	CO_2 treatment (µatm)	DIC (µmol kg^{-1})	pH	Total alkalinity (µmol kg^{-1})	pCO_2 (µatm)
T. pseudonana					
N replete	400	2134 ± 4	8.07 ± 0.01	2417 ± 2	392 ± 6
	750	2186 ± 10	7.83 ± 0.01	2350 ± 8	718 ± 20
N limited-1	400	2152 ± 16	8.07 ± 0.01	2437 ± 21	396 ± 3
	750	2291 ± 28	7.86 ± 0.02	2473 ± 22	701 ± 41
N limited-2	400	2184 ± 2	8.07 ± 0.00	2473 ± 2	398 ± 0
	750	2311 ± 19	7.84 ± 0.01	2483 ± 17	747 ± 17
P. tricornutum					
N replete	400	2142 ± 3	8.06 ± 0.01	2423 ± 1	397 ± 6
	750	2156 ± 5	7.87 ± 0.02	2335 ± 12	648 ± 23
N limited-1	400	2160 ± 9	8.07 ± 0.00	2448 ± 0	394 ± 0
	750	2176 ± 0	7.86 ± 0.00	2352 ± 0	665 ± 0
N limited-2	400	2154 ± 4	8.07 ± 0.01	2443 ± 9	390 ± 11
	750	2167 ± 6	7.86 ± 0.01	2343 ± 10	662 ± 14
T. weissflogii					
N replete	400	2178 ± 6	8.03 ± 0.00	2442 ± 6	439 ± 1
	750	2335 ± 5	7.83 ± 0.01	2504 ± 6	773 ± 11
N limited-1	400	2147 ± 10	8.10 ± 0.02	2450 ± 4	366 ± 21
	750	2327 ± 3	7.85 ± 0.01	2507 ± 9	722 ± 19
N limited-2	400	2162 ± 4	8.08 ± 0.01	2456 ± 10	385 ± 9
	750	2244 ± 10	7.86 ± 0.01	2426 ± 7	680 ± 12

Carbonate chemistry in the media

The pH on the total scale (pH_T) of the culture media was monitored daily using a spectrophotometric method (Zhang & Byrne 1996), and drifted by <0.1 units throughout the experimental period. The dissolved inorganic carbon (DIC) concentration was determined by acidification of the samples and subsequent quantification of released CO_2 with a CO_2 analyzer (LI 7000, Apollo SciTech). The CO2Sys program (Pierrot et al. 2006) was used to calculate alkalinity and pCO_2 based on measurements of pH_T and DIC using the carbonic acid dissociation constants of Mehrbach et al. (1973) that were refitted in different functional forms by Dickson & Millero (1987). The carbonate chemistry of the different experimental treatments is shown in Table 2.

Organic C and N content

Samples were collected onto 25 mm pre-combusted GF/F membranes (450°C, 4.5 h) and stored at –80°C prior to further analysis. Before analysis, the filter membranes were dried overnight at 60°C, exposed to fuming HCl for at least 12 h to remove inorganic C, dried overnight again at 60°C, and then packed in tin

cups. The measurement of organic C and N was conducted on a PerkinElmer 2400 Series II CHNS/O Analyzer.

Short-term C uptake

To determine short-term C uptake, 100 µM $NaH^{14}CO_3$ (PerkinElmer) was added to 50 ml of diatom cultures. The cells were then incubated for 20 min under the growth conditions described above. After incubation, the cells were collected onto 1.2 µm polycarbonate membrane filters (Millipore), which were then washed with 0.22 µm-filtered oligotrophic seawater and placed on the bottom of scintillation vials. The filters were acidified to remove inorganic C by adding 500 µl of 2% HCl and incubated overnight. The radioactivity was determined using a Tri-Carb 2800TR Liquid Scintillation Analyzer (PerkinElmer).

Active fluorescence

Diatom cells were first dark adapted for 10 min to relax photosynthetic activity, and then active fluorescence characteristics of each sample were determined using a pulse amplified modulated chlorophyll fluorometer (WATER-PAM Chlorophyll Fluorometer, Walz) equipped with Win Control software. Minimum fluorescence (F_o) of the cells was measured with a weak probe pulse, and the maximum fluorescence (F_m) was then measured by applying a saturating light pulse of 4000 µmol photons m^{-2} s^{-1} for 0.8 s. Maximum quantum yield of PSII was estimated as $F_v/F_m = (F_m - F_o)/F_m$. Next, fluorescence ($F$) and maximal fluorescence (F_m') in the presence of ambient light were measured similarly except that the sample was illuminated with continuous actinic light adjusted to approximate the growth irradiance.

A rapid light curve (RLC) was measured at 9 different photosynthetic active radiation (PAR) levels (31, 154, 237, 349, 533, 796, 1129, 1579 and 2574 µmol photons m^{-2} s^{-1}) and each PAR level lasted for 10 s, acquiring measurements for fluorescence and maximal fluorescence at each level. The RLC was used to determine the relative electron transport rate (rETR) at growth irradiance ($rETR_{150}$) and the maximal rETR ($rETR_m$). rETR was calculated as: yield × PAR × 0.5 × 0.84, where the yield represents the effective quantum yield of photosystem II (PSII) (i.e. $(F_m' - F)/F_m'$), the coefficient 0.5 takes into account that about 50% of all absorbed quanta reach PSII, and the parameter 0.84 corresponds to the fraction of incident photons absorbed by photosynthetic pigments.

Western blotting

Following collection by gentle filtration onto 1.2 µm polycarbonate membranes (Millipore), 100 ml of the diatom cells from each replicate was snap frozen in liquid nitrogen, and then stored at −80°C for future analysis. Proteins were extracted and denatured in an extraction buffer (2% SDS, 10% glycerol, and 50 mM Tris at pH 6.8; and 1% β-mercaptoethanol was added after protein quantification) by heating at 100°C for 5 min. After centrifugation to remove the insoluble fraction, the total protein in the supernatant was quantified using the bicinchoninic acid assay (No. 23227, Pierce, Thermo Scientific). The protein sample was separated on a 12% SDS polyacrylamide gel for 20 min at 80 V, followed by 30 min at 140 V for the assay of PsbA (the D1 protein of PSII) and PsaC (a core subunit of photosystem I [PSI]) and 60 min at 100 V for the assay of nitrate reductase (NR) and RbcL (the large subunit of RuBisCO) in 1 × SDS running buffer. After gel separation, proteins were then transferred onto PVDF membranes in ice-cold transfer buffer (25 mM Tris, 192 mM glycine and 10% methanol) for 1 h at 30 mA. The membrane was then blocked for 1 h in TBST buffer (Tris-buffered saline with 0.25% Tween 20) containing 5% nonfat milk, followed by 1 to 2 h incubation with the primary antibody (Agrisera Antibodies: RbcL, Art. no. AS03 037; PsbA, Art. no. AS05 084; PsaC, Art. no. AS04 042S; NR, Art. no. AS08 310) and subsequently washed with TBST buffer. The membrane was then probed with alkaline phosphatase-conjugated goat anti-rabbit IgG for 1 h. Following 3 rinses with TBST buffer, protein bands on the membrane were visualized with NBT/BCIP (No. 11681451001, Roche) in PhoA buffer (100 mM Tris, 100 mM NaCl, and 10 mM $MgCl_2$, pH 9.5) and quantified by densitometry.

RNA isolation and standard preparation

Total RNA was extracted using Trizol reagent (Invitrogen) following the manufacturer's instruction. The extracted RNAs were treated with DNase (M6101, Promega) to eliminate genomic DNA contamination.

Standards for qPCR were generated as described previously (Shi et al. 2015). Briefly, the extracted RNA was reverse-transcribed to cDNA using mix-

tures of oligo $(dT)_{20}$ primer (5′-TTT TTT TTT TTT TTT TTT TT-3′) and random primer (5′-NNN NNN-3′) with M-MLV reverse transcriptase (BGI). The cDNA amplicon of the genes of interest were PCR amplified. The primer sequences of each gene were obtained from the literature or designed at the Genscript website and checked for validity using the Primer-Blast tool in NCBI (Table 3). Amplified products were separated using gel electrophoresis, purified and inserted into pMD 18-T vectors (T6011, Takara Bio), which were transformed into DH5α *Escherichia coli* competent cells. Plasmid DNA from positive clones was extracted, purified, quantified using UV1800 (Shimazu), and sequenced by Invitrogen Biotechnology (Shanghai).

Quantitative PCR (qPCR)

Genes that are representative of photorespiration, the CCM, and respiration were selected to quantify the changes of these metabolic pathways in response to elevated pCO_2 under the different N conditions (Table 3). Among them, the glycine decarboxylase T-protein (GDCT) and phosphoglycolate phosphatase (PGP) are involved in photorespiration, carbonic anhydrases (CAs) are essential genes in the CCM, and cytochrome c oxidase (COX) is an important protein involved in the respiratory electron transport chain.

Total RNA was extracted from each sample, treated with DNase and transcribed to cDNA as described above. All qPCR reactions were carried out on a fluorescent quantitative instrument CFX 96 TOUCH (Bio-Rad Laboratories). A SYBR Green I master mix (No. 204007, Zhishan Biotech) was used for qPCR in 15 µl reaction systems containing 3 µl of diluted cDNA, 0.2 mM dNTPs, 200 nM each of forward and reverse primers (Table 3), with the following thermal cycle program: 95°C for 3 min, followed by 40 cycles of 95°C for 15 s, 60°C for 25 s and 72°C for 20 s. Standards corresponding to between 1 to 10^5 ng μl^{-1} per

Table 3. Gene information and qPCR primer sequences of enzymes involved in key metabolic processes of the diatoms *Thalassiosira pseudonana*, *Phaeodactylum tricornutum*, and *T. weissflogii*

Diatom Enzymes	Gene ID	Size (bp)	Primer Name	Sequence (5′–3′)
T. pseudonana				
Phosphoglycolate phosphatase (PGP)	7451838	207	PGP-F PGP-R	TTG CCT GGT GTG GAT GTC ATT TCT TCG GCG GGA ACG
Carbonic anhydrase (CA)	7442183	308	CA-F CA-R	ATG GCA ACG GTC CTC ATG GAA ATG TTG AAT GTC TTG TCC GCC AAG CGT AGT GAA A
Cytochrome oxidase subunit1 (COX1)	3671146	196	COX1-F COX1-R	TGT CGA TGG GTG CAG TAT TT GCG TCA GGA TAA TCA GGG AT
Actin	7449411 (XM_002294881)[a]	162	Actin-F Actin-R	ACT GGA TTG GAG ATG GAT GG CAA AGC CGT AAT CTC CTT CG
P. tricornutum				
Phosphoglycolate phosphatase (PGP)	7204994	231	PGP-F PGP-R	CGA CGC TCA ATT TAT AGC CA AAC AGC ACA TCC GTA TCC AA
Carbonic anhydrase (CA)	15778654	181	CA-F CA-R	TCC GCA ACT ACT GCT CTG TC CAT CGA CGC ATC CAA TGT A
Cytochrome oxidase subunit1 (COX1)	324309727	106	COX1-F COX1-R	TGT CGA TGG GTG CAG TAT TT GCG TCA GGA TAA TCA GGG AT
Actin	57864661 (AY729845)[a]	242	Actin-F Actin-R	TGA CAG AGC GTG GTT ACT CG ACC ATC CAT CTC CAA ACC AC
T. weissflogii				
Glycine decarboxylaseT-protein subunit (GDCT)	7205049	252	GDCT-F GDCT-R	AAA CTC ATC TCC GAC CCA AC CAT GAT ACC AAC ACG CTT CC
Carbonic anhydrase (CA)	34014271	199	CA-F CA-R	GGA GAA GTG CAG GAT GGA TT GGT TGC AGA ATA CAC CAT CG
Cytochrome oxidase subunit1 (COX1)	257799001	197	COX1-F COX1-R	GTG TTG GAA CTG GTT GGA CA CCA TAC AAA TAG AGG AAG ATT ATG GA
Actin	4138666 (AJ002018)[a]	232	Actin-F Actin-R	ATT CCG GAG ATG GTG TTA CC GCA GCC TTC TTC ATT TCC TC

[a]Accession numbers

well were amplified on the same 96-well plate. Dissociation curve analysis was carried out to confirm that only the targeted PCR product was amplified and detected. The RNA samples were also tested in a qPCR to make sure contaminating DNA was not present in the RNA extract (Parker & Armbrust 2005). In order to correct for differences in cDNA synthesis efficiency, the abundance of each transcript was normalized to the abundance of the actin transcript (McGinn & Morel 2008).

Nitrate reductase (NR) activity

NR activity was assessed using the spectrophotometric method (Berges and Harrison 1995, Lomas 2004, Shi et al. 2015). Briefly, cells were ground thoroughly on ice in homogenization buffer (200 mM phosphate buffer, pH 7.9; 1 mM dithiothreitol; 0.3% w/v polyvinyl pyrrolidone; 0.1% v/v Triton X-100; 3% v/v bovine serum albumin; 5 mM EDTA), followed by centrifugation at 1000 × g for 5 min at 4°C. The resulting supernatant was then added to freshly prepared reaction buffer (20 mM phosphate buffer, pH 7.9; 0.2 mM NADH; 10 mM KNO_3) and allowed to incubate for 30 min at 20°C. After the reactions were terminated, samples were centrifuged at 12 000 × g for 5 min and then 0.83 mM phenazine methosulfate was added to the supernatant to oxidize any residual NADH. The NO_2^- concentration in the supernatant was determined colormetrically after reacting with sulfanilamide and N-(1-naphtyl)-ethylenediamine dihydrochloride for 30 min. The activity of NR was calculated from NO_2^- production during the incubation (after correcting for NO_2^- contamination by subtraction with blanks) and normalized to the total number of cells.

Energy budgets

The responses of photosynthesis and net C assimilation of the diatoms to ocean acidification under N-replete and N-limiting conditions were evaluated using a cellular energy budget approach as described in Shi et al. (2015). Briefly, the budgets took into account energy generation from PSII (calculated as PsbA × rETR) and energy expenditures on the CCM, photorespiration, NO_3^- reduction, and respiration, and all energy generation or expenditures at 750 µatm CO_2 were normalized to those at 400 µatm CO_2 to predict changes of photosynthetic and net C assimilation rates.

Data analysis

Data were analyzed using SPSS Statistics 19.0 (IBM Software) for significance of differences between the 400 and 750 µatm treatment groups using a *t*-test. A significant level of $p < 0.05$ was applied, except as noted where significance was even greater.

RESULTS

Growth and elemental composition

The N-replete cells were harvested in the mid-exponential growth phase when less than two-thirds of the initially added NO_3^- (100 µM) in the media had been consumed. For N-limited cultures, the initial concentration of NO_3^- was 15 µM and NO_3^- depletion (< 0.1 µM) occurred at 48 h, 48 h, and 36 h before reaching the N limited-1 stage in the *Thalassiosira pseudonana*, *Phaeodactylum tricornutum*, and *T. weissflogii* cultures, respectively (Fig. A1). The specific growth rates at the N limited-1 stage were detectable for *P. tricornutum* and *T. weissflogii*, although they were much lower than those of the exponential growth phase (Table 4), suggesting that the cells were still dividing and the biomass was still increasing. The cells at the N limited-2 stage were under more severe N deprivation and growth was not detectable.

In N-replete cultures, elevated pCO_2 significantly increased the growth rate of *P. tricornutum* by 6% ($p < 0.05$), while those of *T. pseudonana* and *T. weissflogii* were not affected (Table 4). As the pCO_2 rose from 400 to 750 µatm, the cellular C quota increased significantly in *T. pseudonana* and *P. tricornutum* (by 15 and 17%, respectively, $p < 0.05$) but not in *T. weissflogii*. In contrast, the cellular N quota in all 3 diatom species did not show a marked response to increasing CO_2 (Table 4). In *P. tricornutum* and *T. weissflogii*, particulate C:N ratios were slightly but not significantly higher ($p > 0.05$) under high pCO_2, which was mainly attributed to the increases in cellular C quota.

When NO_3^- was limiting, the cellular C quota increased significantly by about 20% in *T. pseudonana* and up to 13% in *T. weissflogii* ($p < 0.05$), but slightly decreased in *P. tricornutum* at high CO_2 (Table 4). Cellular N quotas were generally lower in N-limited diatoms at high CO_2, and the difference was statistically significant in *P. tricornutum* and *T. weissflogii* ($p < 0.05$). As a result, the C:N ratios increased with increasing pCO_2 in all 3 diatom species under N-limiting conditions, particularly in *T.*

Table 4. The growth rate, cellular C quota and N quota, and the C:N ratio of the diatoms *Thalassiosira pseudonana*, *Phaeodactylum tricornutum*, and *T. weissflogii* acclimated to 2 different pCO_2 levels (400 and 750 µatm) under different N nutritional conditions (N nutri. cond.). N limited-1 and N limited-2 represent cultures harvested at 36 and 72 h after entering the stationary phase, respectively (Fig. A1 in Appendix 1). Data are mean ± SD (n = 3). Asterisks indicate significant difference between CO_2 treatments (*t*-test): $^{*}p < 0.05$, $^{**}p < 0.01$

Diatom N nutri. cond.	CO_2 treatment (µatm)	Growth rate (µ d^{-1})	C quota (pmol $cell^{-1}$)	N quota (pmol $cell^{-1}$)	C:N
T. pseudonana					
N replete	400	1.90 ± 0.08	0.91 ± 0.08	0.096 ± 0.005	10.5 ± 0.4
	750	1.85 ± 0.03	1.05 ± 0.09	0.103 ± 0.007	10.2 ± 0.2
N limited-1	400	~0	0.92 ± 0.02	0.050 ± 0.005	19.2 ± 0.9
	750	~0	1.10 ± 0.11*	0.048 ± 0.002	22.0 ± 1.3*
N limited-2	400	~0	0.99 ± 0.07	0.039 ± 0.004	22.6 ± 0.7
	750	~0	1.19 ± 0.09*	0.040 ± 0.008	24.3 ± 0.9
P. tricornutum					
N replete	400	1.50 ± 0.02	1.33 ± 0.01	0.20 ± 0.01	6.7 ± 0.2
	750	1.59 ± 0.04*	1.56 ± 0.07**	0.22 ± 0.02	7.0 ± 0.5
N limited-1	400	0.19 ± 0.03	0.84 ± 0.02	0.040 ± 0.006	21.4 ± 1.8
	750	0.19 ± 0.04	0.82 ± 0.01	0.038 ± 0.011	25.7 ± 4.3
N limited-2	400	~0	0.95 ± 0.01	0.042 ± 0.002	22.8 ± 1.1
	750	~0	0.93 ± 0.02	0.037 ± 0.001*	25.2 ± 0.3*
T. weissflogii					
N replete	400	1.01 ± 0.04	7.91 ± 0.24	0.98 ± 0.09	8.1 ± 0.5
	750	0.99 ± 0.01	8.58 ± 0.22*	1.01 ± 0.06	8.5 ± 0.3
N limited-1	400	0.10 ± 0.03	7.57 ± 0.22	0.32 ± 0.03	23.7 ± 1.8
	750	0.11 ± 0.03	8.55 ± 0.32*	0.26 ± 0.01*	32.1 ± 2.9**
N limited-2	400	~0	7.55 ± 0.16	0.22 ± 0.03	33.0 ± 4.1
	750	~0	7.92 ± 0.38	0.19 ± 0.01	40.2 ± 0.8*

weissflogii as the increase was significant at both N limited-1 and N limited-2 ($p < 0.05$; Table 4).

Short-term C uptake

At high CO_2, the short-term C uptake rate increased by 15 and 26%, respectively, in N-replete *T. pseudonana* and *P. tricornutum* ($p < 0.05$), whereas it changed negligibly in N-replete *T. weissflogii* (Fig. 1). When N was limiting, high CO_2 slightly increased the rate of short-term C uptake of *T. pseudonana* and *T. weissflogii* by 5 to 20% but decreased that of *P. tricornutum* by 5 to 15%, although the changes were not statistically significant.

Active fluorescence

F_v/F_m, $rETR_{max}$, and $rETR_{150}$ were all much higher in N-replete cells than in N-limited ones (Table 5). Elevated pCO_2 did not cause significant changes in F_v/F_m in *T. pseudonana*, *P. tricornutum* and *T. weissflogii*. When

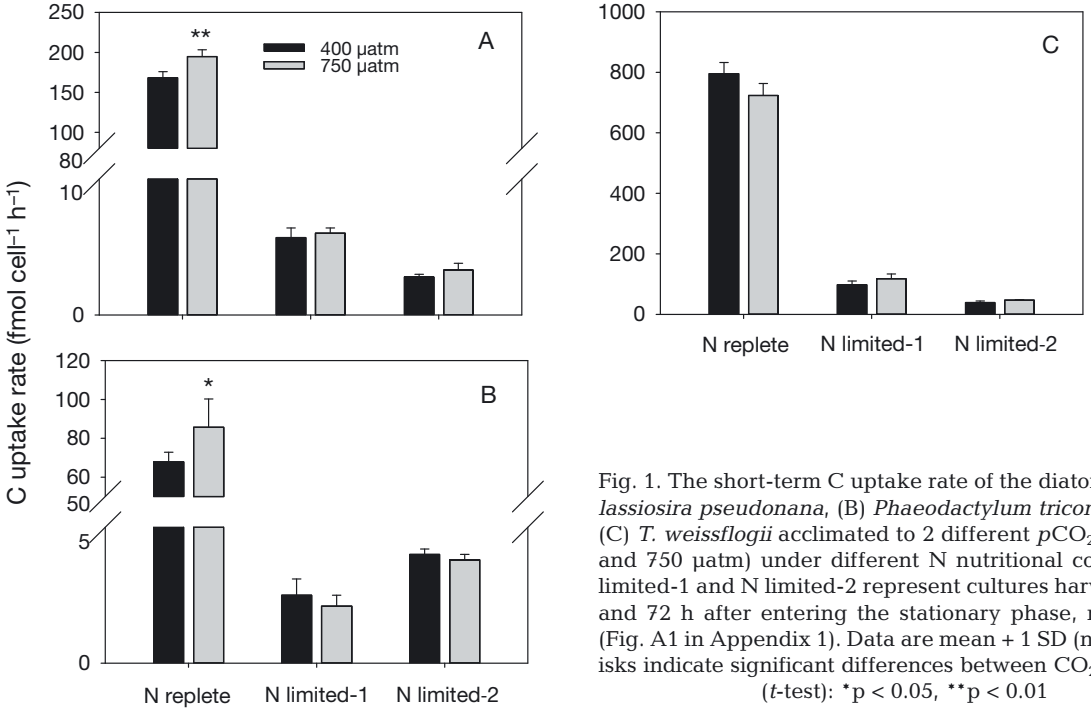

Fig. 1. The short-term C uptake rate of the diatoms (A) *Thalassiosira pseudonana*, (B) *Phaeodactylum tricornutum*, and (C) *T. weissflogii* acclimated to 2 different pCO_2 levels (400 and 750 µatm) under different N nutritional conditions. N limited-1 and N limited-2 represent cultures harvested at 36 and 72 h after entering the stationary phase, respectively (Fig. A1 in Appendix 1). Data are mean + 1 SD (n = 3). Asterisks indicate significant differences between CO_2 treatments (*t*-test): $^{*}p < 0.05$, $^{**}p < 0.01$

Table 5. Photochemical quantum yield of photosystem II (F_v/F_m), relative electron transport rate at the growth irradiance ($rETR_{150}$), and the maximal rate of relative electron transport at the saturating irradiance ($rETR_{max}$) of the diatoms *Thalassiosira pseudonana*, *Phaeodactylum tricornutum*, and *T. weissflogii* acclimated to 2 different pCO_2 levels (400 and 750 µatm) under different N nutritional conditions (N nutri. cond.). N limited-1 and N limited-2 represent cultures harvested at 36 and 72 h after entering the stationary phase, respectively (Fig. A1 in Appendix 1). Data are mean ± SD (n = 3). Asterisks indicate significant difference between CO_2 treatments (*t*-test): *p < 0.05, **p < 0.01, ***p < 0.001

Diatom N nutri. cond.	CO_2 treatment (µatm)	F_v/F_m	$rETR_{150}$	$rETR_{max}$
T. pseudonana				
N replete	400	0.61 ± 0.02	27.8 ± 0.4	127.3 ± 0.6
	750	0.57 ± 0.02	26.9 ± 0.8	126.5 ± 3.5
N limited-1	400	0.40 ± 0.04	21.9 ± 0.9	96.3 ± 3.4
	750	0.34 ± 0.05	21.8 ± 1.4	97.8 ± 4.8
N limited-2	400	0.37 ± 0.04	19.4 ± 1.6	79.4 ± 3.6
	750	0.25 ± 0.01*	17.0 ± 1.4	72.5 ± 6.5
P. tricornutum				
N replete	400	0.41 ± 0.03	28.1 ± 1.5	105.4 ± 3.4
	750	0.43 ± 0.04	27.9 ± 1.1	120.7 ± 5.3*
N limited-1	400	0.31 ± 0.01	18.0 ± 1.1	82.4 ± 4.4
	750	0.31 ± 0.01	18.7 ± 1.8	86.5 ± 5.8
N limited-2	400	0.32 ± 0.02	17.5 ± 0.2	79.4 ± 3.6
	750	0.33 ± 0.02	18.0 ± 0.6	72.5 ± 6.5
T. weissflogii				
N-replete	400	0.50 ± 0.01	26.1 ± 1.6	97.1 ± 3.3
	750	0.55 ± 0.04	27.2 ± 1.0	111.6 ± 12.2
N-limited-1	400	0.33 ± 0.03	18.6 ± 0.6	44.5 ± 3.2
	750	0.38 ± 0.03	20.1 ± 1.3	64.9 ± 6.2**
N-limited-2	400	0.14 ± 0.01	8.3 ± 0.4	13.9 ± 1.0
	750	0.20 ± 0.04	10.9 ± 1.1*	24.4 ± 1.7***

N was replete, $rETR_{max}$ was slightly higher at high CO_2 in *P. tricornutum* and *T. weissflogii*. When N was limiting, $rETR_{max}$ and $rETR_{150}$ of *T. weissflogii* responded positively to increased CO_2 ($p < 0.01$), whereas these parameters did not change markedly in *T. pseudonana* and *P. tricornutum*.

Protein expression and gene transcription levels

The abundance of the photosynthetic proteins RbcL, PsaC, and PsbA all declined as N became limiting (Fig. 2). In N-replete cells, the expression of RbcL was consistently induced at high CO_2, although the increase was not statistically significant (Fig. 2A,D,G). CO_2 treatment did not change the protein expression levels of PsaC and PsbA in all diatoms under N-replete conditions (Fig. 2).

In N-limited *T. pseudonana*, increased pCO_2 had more profound effects on the expression of PsaC and PsbA than that of RbcL, with PsaC and PsbA being down-regulated by 19 to 60% and 12 to 20% ($p < 0.05$), respectively (Fig. 2A–C). In N-limited *P. tricornutum*, increased pCO_2 significantly reduced the protein abundance of RbcL by approximately 40% ($p < 0.05$), PsbA by 25% ($p < 0.01$) and PsaC by about 20% ($p < 0.05$) (Fig. 2D–F). The protein expression of RbcL was not affected by pCO_2 in N-limited *T. weissflogii*, whereas those of PsaC and PsbA decreased (< 25% for PsaC and < 10% for PsbA, $p > 0.05$) at high CO_2 (Fig. 2G-I).

The gene transcription of a CA, which is essential in the CCM, decreased significantly at high CO_2 in both N-replete and N-limited *T. pseudonana*, *P. tricornutum* and *T. weissflogii* ($p < 0.05$; Fig. 3A,D,E), indicating the down-regulation of the CCM in all 3 diatom species at high CO_2. The gene transcription of the cytochrome oxidase subunit1 (COX1), which plays an important role in respiratory electron transfer, was not affected by CO_2 concentration when N was sufficient (Fig. 3B,E,H). In contrast, in N-limited *T. pseudonana*, *P. tricornutum* and *T. weissflogii*, increased CO_2 inhibited the transcription of the *COX1* gene by 20 to 27, 20 to 32 and 35 to 70%, respectively. *PGP* and *GDCT* are representative photorespiration genes in diatoms. The transcription levels of *PGP* in *T. pseudonana* and *P. tricornutum* and *GDCT* in *T. weissflogii* generally, but not in all cases significantly, decreased at high CO_2 (Fig. 3C,F,I), suggesting reduced photorespiration at elevated CO_2.

NR expression and activity

NR catalyzes the reduction of NO_3^- to nitrite (NO_2^-), which is an essential step in NO_3^- assimilation. The activity of NR has often been used as an index for NO_3^- uptake for diatoms (Berges et al. 1995). Here, the effect of acidification on NR was characterized at both protein expression and enzymatic activity levels. Elevated pCO_2 generally did not affect the protein expression and activity of NR in N-replete *T. pseudonana*, *P. tricornutum*, and *T.*

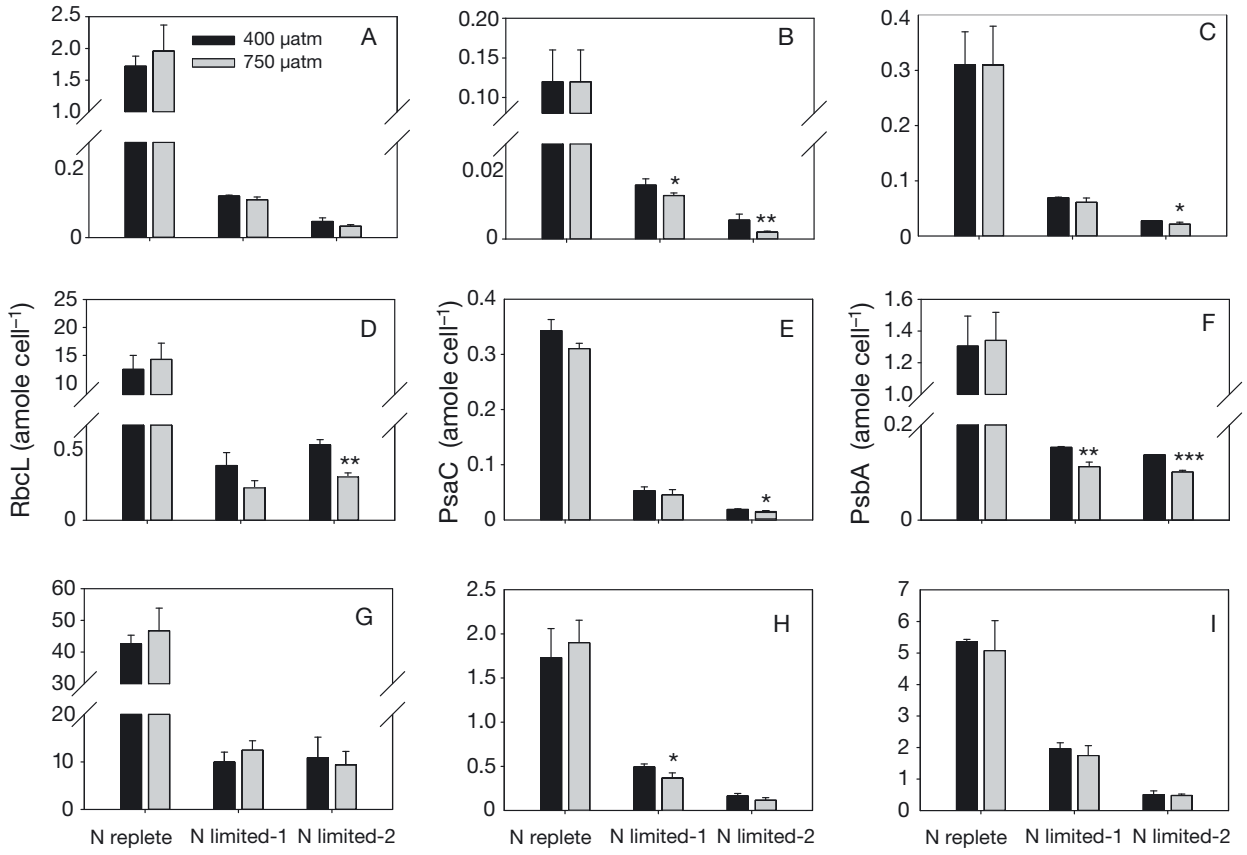

Fig. 2. The expression of photosynthetic proteins (A,D,G) RbcL, (B,E,H) PsaC, and (C,F,I) PsbA in the diatoms (A–C) *Thalassiosira pseudonana*, (D–F) *Phaeodactylum tricornutum*, and (G–I) *T. weissflogii* acclimated to 2 different pCO_2 levels (400 and 750 µatm) under different N nutritional conditions. N limited-1 and N limited-2 represent cultures harvested at 36 and 72 h after entering the stationary phase, respectively (Fig. A1 in Appendix 1). Data are means + 1SD (n = 3). Asterisks indicate significant differences between CO_2 treatments (*t*-test): *p < 0.05, **p < 0.01, ***p < 0.001

weissflogii (Fig. 4). However, NR abundance and activity were reduced by increased CO_2 in N-limited cells, and the reduction was statistically significant in *P. tricornutum* (on average decreased by 72% and 48%, respectively) and *T. pseudonana* (average decrease 28% and 35%, respectively) but not in *T. weissflogii* (average decreased 16% and 6%, respectively) (Fig. 4).

DISCUSSION

The physiology of marine phytoplankton is dynamic and highly responsive to the changing environment, which is reflected in the complex reallocation of cellular energy and resources among metabolic processes to optimize growth (Halsey & Jones 2015). By quantitatively assessing key cellular processes involved in phytoplankton energy metabolism, Shi et al. (2015) demonstrate that an energy budget incorporating energy production and expenditure associated with the most relevant processes can be a useful approach for predicting the response of phytoplankton photosynthesis and growth to environmental perturbations (e.g. ocean acidification). In our study, we used this approach to evaluate the impacts of different N nutritional conditions (N-replete vs. N-limiting) on the responses in energy metabolism and growth of 3 model diatom species to ocean acidification.

Energy metabolism in N-replete diatoms

The gene transcription of the CA, an essential enzyme in the CCM (Roberts et al. 1997, Satoh et al. 2001), negatively correlated with pCO_2 in our study, which agrees well with previous observations (e.g. McGinn & Morel 2008), suggesting CCM down-regulation at elevated CO_2. It has been suggested that the energy saved from CCM down-regulation

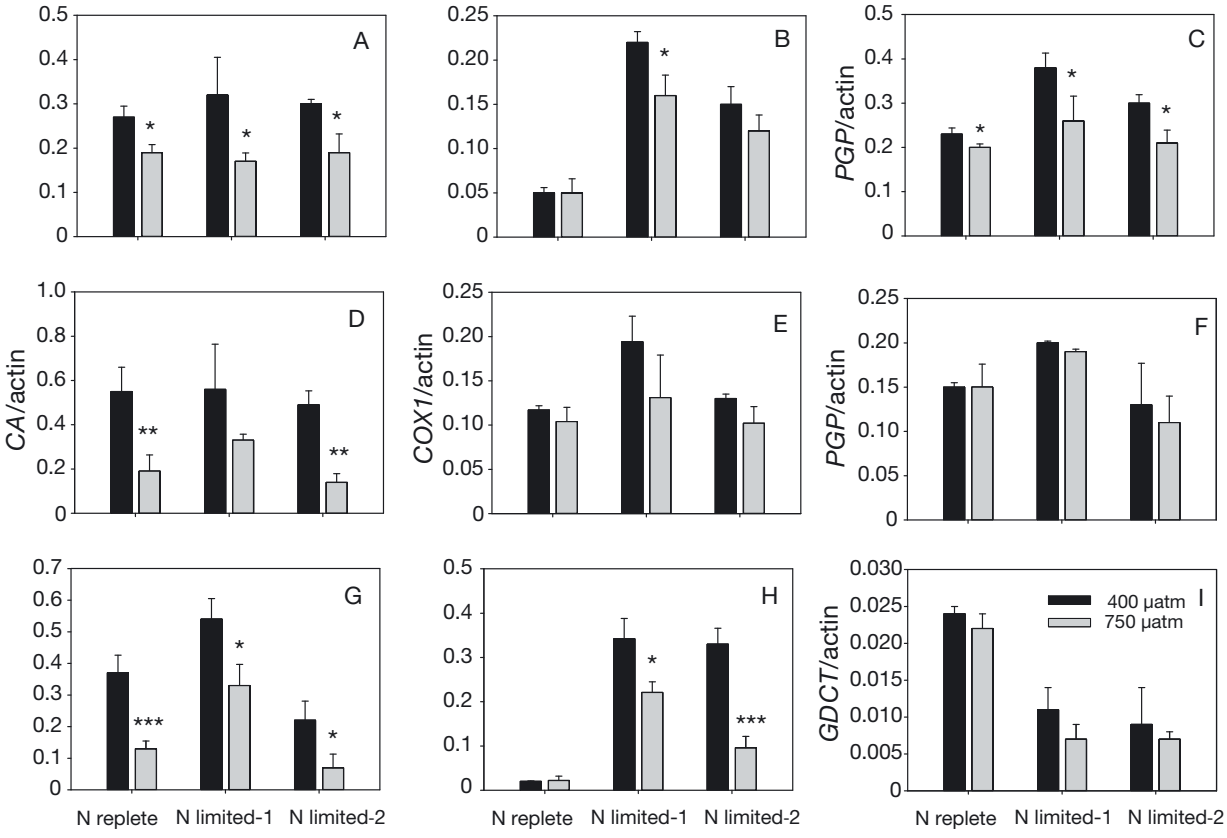

Fig. 3. Ratios of copy numbers of (A,D,G) carbonic anhydrase (*CA*), (B,E,H) cytochrome oxidase subunit1 (*COX1*), (C,F) phosphoglycolate phosphatase (*PGP*), and (I) glycine decarboxylase T-protein (*GDCT*) mRNA to actin mRNA in the diatoms (A–C) *Thalassiosira pseudonana*, (D–F) *Phaeodactylum tricornutum* and (G–I) *T. weissflogii* acclimated to 2 different pCO_2 levels (400 and 750 µatm) under different N nutritional conditions. N limited-1 and N limited-2 represent cultures harvested at 36 and 72 h after entering the stationary phase, respectively (Fig. A1 in Appendix 1). Data are means + 1 SD (n = 3). Asterisks indicate significant differences between CO_2 treatments (*t*-test): *p < 0.05, **p < 0.01, ***p < 0.001

can be reallocated to support increased rates of photosynthesis and growth (Rost et al. 2008). In diatoms, the energy saved from the down-regulation of the CCM by doubling of ambient CO_2 concentration is estimated to increase the C fixation rate by 2 to 10% (Hopkinson et al. 2011). Photorespiration in diatoms is energetically expensive requiring 872 kJ per mole C fixed (Raven et al. 2000, Hennon et al. 2015), and its genes are in the same CO_2-responsive cluster as CCM genes and hence they are co-regulated in response to changes in CO_2 (Hennon et al. 2015). In our study, changes in the transcription of photorespiration genes *GDCT* or *PGP* in response to increasing pCO_2 were minor in the N-replete diatoms (Fig. 3), as previously observed (Roberts et al. 2007, Shi et al. 2015), and thus the estimated effect of down-regulation of photorespiration on the photosynthetic rate was negligible (0 to 1%; Table 6). It should be noted that in the present study NO_3^- was used as the sole N source. In the future ocean, however, phytoplankton will likely be growing on increasing ammonium (NH_4^+) due to reduced nitrification, decreased NO_3^- flux from deep waters and enhanced anthropogenic NH_4^+ deposition as a result of global climate change (Doney 2006, Duce et al. 2008, Beman et al. 2011). Consequently, the extra energy expended on photorespiration for a shift in N source from NO_3^- to NH_4^+ could dominate the energetic savings from down-regulation of photorespiration at high CO_2 (Shi et al. 2015), thereby affecting photosynthesis negatively.

The energy saved from changes in NO_3^- reduction was also small in all 3 diatom species, as previously observed (Shi et al. 2015), and estimated potential changes in photosynthetic rates from reallocation of this energy were trivial (0 to 2%; Table 6). In terms of energy generation, relative photon flux rates from PSII, which were estimated using PsbA × $rETR_{150}$, did not change significantly in N-replete cells grown at elevated CO_2 and were estimated to decline by only 0 to 3% (Table 6). Therefore, considering energetic reallocation among all these metabolic pathways, the

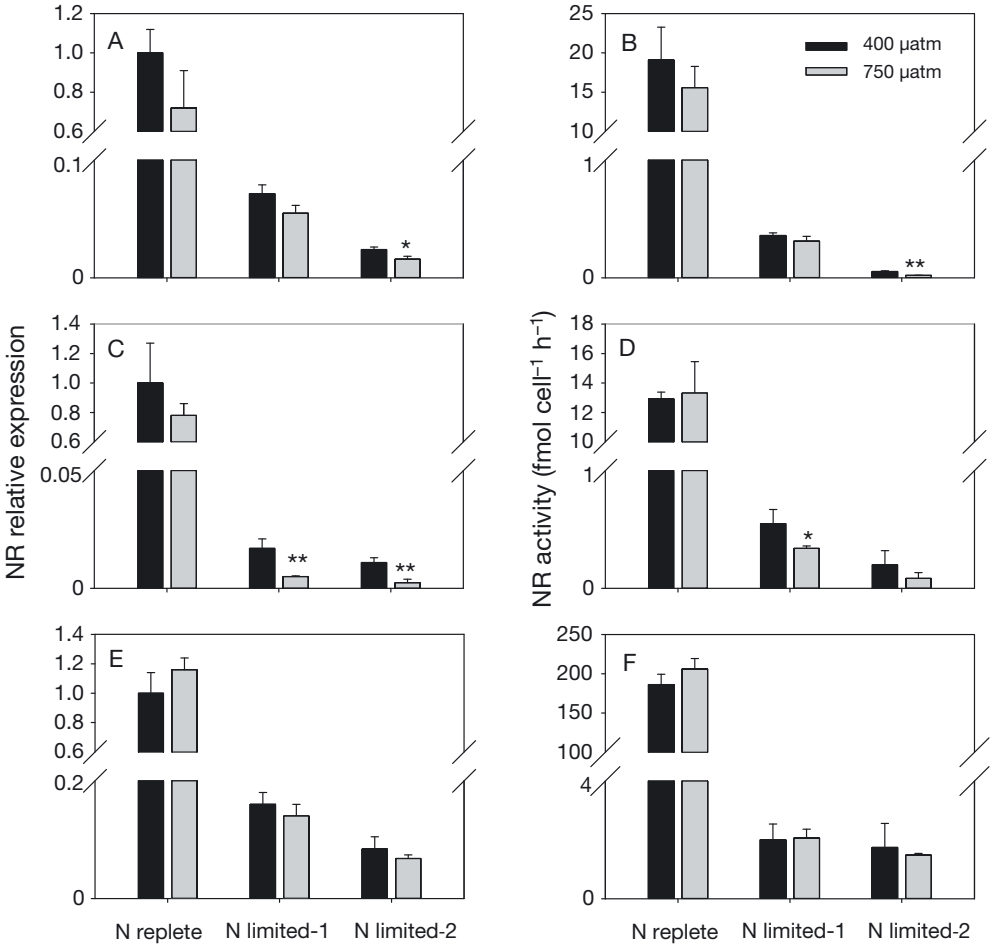

Fig. 4. The relative expression (left panels) and activity (right panels) of nitrate reductase (NR) in the diatoms (A,B) *Thalassiosira pseudonana*, (C,D) *Phaeodactylum tricornutum* and (E,F) *T. weissflogii* acclimated to 2 different pCO_2 levels (400 and 750 µatm) under different N nutritional conditions. N limited-1 and N limited-2 represent cultures harvested at 36 and 72 h after entering the stationary phase, respectively (Fig. A1 in Appendix 1). Data are means + 1 SD (n = 3). Asterisks indicate significant differences between CO_2 treatments (*t*-test): *p < 0.05, **p < 0.01

photosynthetic rate was estimated to increase by 1 to 12% at high pCO_2 in N-replete diatoms (Table 6). This enhancement was generally in agreement with the increase in the short-term C uptake rate of N-replete *Thalassiosira pseudonana*, *Phaeodactylum tricornutum*, and *T. weissflogii* (i.e. 0 to 26%) at elevated pCO_2 (Fig. 1).

In all 3 N-replete diatoms, respiration, which was represented by the transcription of *COX1* gene, did not change significantly at elevated CO_2 (Fig. 3B,E,H) and hence changes in respiration were not predicted to alter net C assimilation substantially (Table 6). As a result, the net C assimilation rate was predicted to increase by 1 to 8%, 8 to 16% and 0 to 10% at high CO_2 in N-replete *T. pseudonana*, *P. tricornutum*, and *T. weissflogii*, respectively. In good agreement with these predictions, the measured net C fixation rate (calculated as growth rate × C quota) of *T. pseudonana*, *P. tricornutum*, and *T. weissflogii* increased by approximately 12, 24, and 8%, respectively, at high CO_2.

Overall, the effect of increasing CO_2 on the N-replete diatoms observed here was small. Among the 3 diatoms, the positive effects of elevated CO_2 on net C fixation were more profound in N-replete *P. tricornutum* than in N-replete *T. pseudonana* and *T.weissflogii*, which was mainly due to the energetic contribution by the down-regulation of respiration.

Energy metabolism in N-limited diatoms

Comparing the responses of N-replete and N-limited cells to rising CO_2 revealed that the behavior of

Table 6. Prediction of changes (%) of photosynthetic rate and net C assimilation by *Thalassiosira pseudonana*, *Phaeodactylum tricornutum*, and *T. weissflogii* at 750 µatm relative to 400 µatm CO_2 using an energy budget incorporating energy production from PSII and energy expenditures on the CO_2 concentration mechanism (CCM), photorespiration, NO_3^- reduction and respiration, calculated according to (Shi et al. 2015). N-limited (N lim.) values shown are the average of values for N limited-1 and N limited-2 treatments; N rep.: N replete

	T. pseudonana		*P. tricornutum*		*T. weissflogii*	
	N rep.	N lim.	N rep.	N lim.	N rep.	N lim.
Relative change in PSII photon flux rate[a]	–3	–14	0	–24	–2	3
Contribution to photosynthetic rate by down-regulation of CCM	2 to 10	2 to 10	2 to 10	2 to 10	2 to 10	2 to 10
Contribution to photosynthetic rate by down-regulation of photorespiration[b]	1	3	0	1	1	4
Contribution to photosynthetic rate by change in nitrate reduction[c]	1	1	2	1	0	0
Predicted relative change of photosynthetic rate[d]	1 to 8	–9 to 0	4 to 12	–20 to –12	1 to 9	9 to 17
Contribution to net carbon fixation by change in respiration[e]	0	8	4	9	–1	16
Predicted relative change of net carbon fixation[f]	1 to 8	–1 to 8	8 to 16	–11 to –3	0 to 10	25 to 33

[a]Calculated as the percentage change in rETR150 × PsbA at 750 µatm relative to 400 µatm CO_2. The values of rETR150 and PsbA are from Table 5 and Fig. 2, respectively. Doubling pCO_2 down-regulates CCM and the energy saved will contribute to the photosynthetic rate by 2 to 10% (Hopkinson et al. 2011)
[b]Calculated as relative change of the expression of *PGP*/*GDCT* genes × (872 kJ mol C^{-1} × 7%)/590 kJ mol C^{-1} (Shi et al. 2015). The transcription levels of *PGP*/*GDCT* genes are from Fig. 3
[c]Calculated as relative change of NR expression × (288 kJ mol N^{-1}/ C:N ratio)/590 kJ mol C^{-1} (Shi et al. 2015). The relative change of NR expression was calculated using the values in Fig. 4
[d]Sum of relative change in photon flux rate, contribution to the photosynthetic rate by down-regulation of CCM, photorespiration and nitrate reduction
[e]Assuming one-third of the carbon fixed by photosynthesis is respired (Losh et al. 2013), contribution to net carbon fixation by decrease in respiration was calculated as relative change of the *COX1* gene expression divided by 3
[f]Predicted relative change of net carbon assimilation is the sum of relative change of the photosynthetic rate and respiration

some metabolic systems were very similar regardless of N-condition, such as the CCM and photorespiration (Fig. 3), whereas other key energy metabolism processes, e.g. light harvesting and respiration, were differently affected by increased CO_2 under the different N nutritional conditions (Figs. 3 & 4). When N was replete, the gene transcription and expression of proteins involved in photosynthesis (PsaC and PsbA) and respiration (COX1) were virtually insensitive to the CO_2 concentration change. In contrast, when N was limiting, increased CO_2 had pronounced effects on the expression of these genes or proteins. For instance, in general PsbA and PsaC were reduced significantly at elevated pCO_2 in the N-limited cultures (Fig. 2). The $rETR_{150}$ of N-limited *T. weissflogii* increased at high CO_2, whereas changes in $rETR_{150}$ in N-limited *T. pseudonana* and *P. tricornutum* were not noticeable (Table 5). Assuming the portion of the active PSII center remained unchanged at different CO_2 concentrations, the estimated energy generation rates from PSII (as PsbA × $rETR_{150}$) at higher CO_2 were 14 and 24% lower in *T. pseudonana* and *P. tricornutum*, respectively, and increased slightly (3%) in *T. weissflogii* under N-limiting conditions (Table 6).

In our study, the expression and activity of NR decreased at high CO_2, particularly under N-limiting conditions, suggesting that N utilization was impaired in N-limited diatoms at high CO_2 (Fig. 4, Table 4). Since NO_3^- reduction is energy consuming and requires 288 kJ per mole NO_3^- reduced (Falkowski & Raven 2007), the decrease of NO_3^- assimilation at elevated CO_2 can save energy, which, albeit being rather limited (Table 6), could be reallocated to other metabolic processes. Incorporating energy production from PSII and energy expenditures on the CCM, photorespiration and NR, the resulting photosynthetic rate was predicted to decrease by 0 to 9% and 12 to 20% in *T. pseudonana* and *P. tricornutum*, respectively, and to increase by 9 to 17% in *T. weissflogii* at high CO_2 under N-limiting conditions (Table 6). In comparison, the measured short-term ^{14}C uptake rate increased by 5 to 17% in *T. pseudonana*, decreased by 5 to 16% in *P. tricornutum* and increased by 19 to 20% in *T. weissflogii* (Fig. 1). The predicted values agree well with the

experimental observations for *P. tricornutum* and *T. weissflogii*. However, they are off for *T. pseudonana*, which may be due to an underestimation of energy generation rates by PSII under high CO_2 conditions using PsbA protein content as a proxy for PSII in active state (Wu et al. 2011, Li et al. 2015), or to the fact that cells were not in steady-state under N-limiting conditions, which the energy budget assumes.

In the present study, when N was limiting, the transcription of the respiration gene *COX1* was down-regulated markedly in all 3 diatom species (Fig. 3B,E,H). Previous studies also show that the respiration rate and transcription of the *COX1* gene decrease at high CO_2 in N-limited *T. pseudonana* (Hennon et al. 2014, 2015). Incorporating the change in photosynthesis and respiration and assuming one-third of the C fixed by photosynthesis is respired (Losh et al. 2013), net C assimilation would change by −1 to 8%, −11 to −3% and 25 to 33% for *T. pseudonana*, *P. tricornutum*, and *T. weissflogii*, respectively, in response to elevated CO_2 (Table 6). Because growth rates of the diatoms were extremely slow (e.g. *P. tricornutum* and *T. weissflogii* at N limited-1) or unmeasurable under N-limiting conditions, their differences between CO_2 treatments were basically indistinguishable (Table 4). Therefore, assuming a constant growth rate in those N-limited cells at the 2 different CO_2 levels, the relative change in net C fixation (as growth rate × C quota) can be represented by that in cellular C quota. It turned out that the experimentally determined changes in cellular C quota of N-limited *T. pseudonana*, *P. tricornutum*, and *T. weissflogii* at high CO_2 were 20, −2 and 10% (Table 4), respectively, which were generally in good agreement with the predictions (Table 6). Overall, among all the key metabolic pathways, the changes in photon flux, the CCM, and respiration were the primary contributors to the effect of elevated CO_2 on the N-limited diatoms.

Elemental stoichiometry

Previous studies on the effects of ocean acidification on marine phytoplankton report varying changes in C:N ratios (e.g. Burkhardt et al. 1999, Li et al. 2012, Reinfelder 2012, Rouco et al. 2013, Eberlein et al. 2016), which may be due to species- and strain-specific responses, differences in experimental conditions, or N nutritional condition. With respect to the impact of N nutritional condition, C:N ratios are generally more sensitive to increasing pCO_2 under N-limiting conditions than under N-replete conditions (e.g. Losh et al. 2012, Eberlein et al. 2016). For instance, in diatom-dominated phytoplankton assemblages off the coast of California, Losh et al. (2012) found that C:N stoichiometry increased slightly at high CO_2 under N-limitation but did not change at high CO_2 when N was sufficient. Similarly, our results showed that in all 3 diatom species, when N was replete the C:N ratio did not change significantly with a doubling of ambient pCO_2, whereas when N was limiting it consistently increased (Table 4).

In the present study, although increased C:N ratio with increasing pCO_2 was common among the N-limited diatoms, the increase was more discernable in *T. weissflogii* than in the other 2 species and cellular C and N quota also showed species-specific changes in response to high CO_2. The increase in C:N ratio was driven largely by the increase in cellular C quota of N-limited *T. pseudonana* and *T. weissflogii*, while it resulted mostly from the decrease in cellular N quota of N-limited *P. tricornutum* (Table 4). The different changes in C and N quota in response to increasing CO_2 among the N-limited diatom species should be a consequence of their varying responses of C and N metabolism. As shown in Fig. 1, the short-term C fixation rate increased slightly with increasing pCO_2 in N-limited *T. pseudonana* and *T. weissflogii*, whereas it slightly decreased at high CO_2 in N-limited *P. tricornutum*, which, as elucidated by the energy budgets (Table 6), was attributed largely to impeded energy generation rates as a result of reduced PSII (decreasing PsbA). Given that under N-limiting conditions the down-regulation of respiration by increasing pCO_2 was more or less comparable among 3 diatom species (Fig. 3B,E,H), net C assimilated decreased slightly in *P. tricornutum* but increased in the other 2 diatom species (Table 4). Differences in C assimilation could also be related to differences in the preference for the source of inorganic C (HCO_3^- vs. CO_2) and to different types of CCM among the diatoms (Giordano et al. 2005, Reinfelder 2011). In terms of N assimilation, its reduction at high CO_2, as indicated by reduced NR expression and activity, was most obvious in *P. tricornutum* among the 3 diatom species under N-limiting conditions (Fig. 4). Consistent with this, the decrease in the abundance of RbcL, PsaC and PsbA at high CO_2 was generally more significant in N-limited *P. tricornutum* than in N-limited *T. pseudonana* and *T. weissflogii* (Fig. 2). RuBisCO and photosynthetic proteins are both abundant proteins in diatoms, accounting for approximately 6% of total protein and 15 to 25% of total cellular N, respectively (Losh et al. 2013, Li et al. 2015). Therefore, down-regulation of these proteins could

reduce the demand for N, in particular when N is in short supply, as in the case of N-limited *P. tricornutum*. Taken together, a relatively stronger decrease in N quota compared to C quota led to increased C:N ratios in N-limited cultures of *P. tricornutum*.

CONCLUSIONS

The response of the metabolic processes of diatom cells to elevated CO_2 was affected by the N nutritional condition. The resulting energy reallocation changed the growth and cellular C and N quota. When N was replete, the down-regulation of the CCM at high CO_2 contributed importantly to the increased growth and photosynthetic rate of diatoms. When N was limiting, besides the changes in CCM and photorespiration, elevated CO_2 had profound effects on photosynthetic photon flux and respiration, and increased the cellular C:N ratio due to either an increase in the cellular C quota or a decrease in the cellular N quota. It is of note that albeit the changes observed here are mostly on the order of 10 to 20%, they could be of consequence as diatoms are known to contribute ~40% of marine primary production (Falkowski et al. 2004). In vast regions of the ocean that are N-limited, the export of C is effectively determined by the C:N ratio of the sinking particles and the input of new N to the surface water. If N input remains unchanged and diatoms fix more C per unit of N in response to elevated pCO_2, it could potentially result in increased C export and thus a negative feedback to the ongoing increase in atmospheric CO_2. Such effects certainly could be modulated by changes in other physical, chemical or biological variables as a result of global change (e.g. temperature, availability of other nutrients and community structures) (Gunderson et al. 2016).

In the present study, the 3 diatom species showed both common (e.g. CCM, photorespiration and respiration) and species-specific (e.g. energy generations under N-limiting conditions) responses of cellular metabolic pathways to ocean acidification. Nevertheless, the energy budget approach based on the key processes involved in C metabolism, N assimilation, photorespiration and respiration did a reasonable job in predicting their respective response of photosynthesis and C fixation to the changing environment under both N-replete and N-limiting conditions. However, it should be noted that in the present study 2 different regulatory levels (i.e. gene transcription and protein expression) of enzymes were used interchangeably to evaluate changes in key metabolic pathways, which were then incorporated into the energy budget to predict the effect of acidification on C fixation and photosynthesis. Previous studies have shown that regulations of a protein at transcriptional, translational and activity levels may not always correlate. For example, RbcL showed a transcript–protein delay of 4 to 6 h in *T. pseudonana* (Granum et al. 2009). In the same diatom species, gene transcription, protein expression and enzyme activity of NR appeared to be highly correlated, as demonstrated here and previously (Vergara et al. 1998, Shi et al. 2015). Decoupling between NR transcription and translation, however, could occur due to changes in N availability, as shown in the diatom *Cylindrotheca fusiformis* (Poulsen & Kroger 2005). Therefore, the energy budget approach should be used carefully when mixing measurements of gene transcription, protein expression and activity as proxies for different metabolic pathways.

In the present study, the N-limited cells were not growing under steady-state conditions. Therefore, future studies with N-limited species cultured using chemostat are needed to further test the use of the energy budget approach. In addition, caution should be taken when applying this approach to predict the response of the phytoplankton community to the changing ocean, as at the community level responses to environmental factors are often linked to change in taxomonic composition (Riebesell et al. 2007) and, moreover, there are certainly differences in responses of cellular energy metabolic pathways among various phytoplankton taxa.

Acknowledgements. We thank Brian Hopkinson (University of Georgia) for his valuable comments during the preparation of this manuscript. We also thank 3 anonymous reviewers for helpful and constructive comments on the manuscript. This work was supported by the National Key Research and Development Program of China (No. 2016YFA0601203), the National Science Foundation of China (No. 41222040), the Fundamental Research Funds for the Central Universities (No. 20720140504), and the Recruitment Program of Global Youth Experts of China. Brian Hopkinson and John Hodgkiss (The University of Hong Kong) are thanked for their assistance with English.

LITERATURE CITED

Beman JM, Chow CE, King AL, Feng Y and others (2011) Global declines in oceanic nitrification rates as a consequence of ocean acidification. Proc Natl Acad Sci USA 108:208–213

Berges JA, Harrison PJ (1995) Nitrate reductase activity quantitatively predicts the rate of nitrate incorporation under steady-state light limitation: a revised assay and

characterization of the enzyme in 3 pieces of marine phytoplankton. Limnol Oceanogr 40:82–93

Berges JA, Cochlan WP, Harrison PJ (1995) Laboratory and field responses of algal nitrate reductase to diel periodicity in irradiance, nitrate exhaustion, and the presence of ammonium. Mar Ecol Prog Ser 124:259–269

Broecker WS (1982) Ocean geochemistry during glacial time. Geochim Cosmochim Acta 46:1689–1705

Burkhardt S, Zondervan I, Riebesell U (1999) Effect of CO_2 concentration on C:N:P ratio in marine phytoplankton: a species comparison. Limnol Oceanogr 44:683–690

Caldeira K, Wickett M (2003) Anthropogenic carbon and ocean pH. Nature 425:365

Dickson AG, Millero FJ (1987) A comparison of the equilibrium constants for the dissociation of carbonic acid in seawater media. Deep-Sea Res 34:1733–1743

Doney SC (2006) Plankton in a warmer world. Nature 444: 695–696

Doney SC, Fabry VJ, Feely RA, Kleypas JA (2009) Ocean acidification: the other CO_2 problem. Annu Rev Mar Sci 1:169–192

Duce RA, LaRoche J, Altieri K, Arrigo KR and others (2008) Impacts of atmospheric anthropogenic nitrogen on the open ocean. Science 320:893–897

Eberlein T, Van de Waal DB, Brandenburg KM, John U, Voss M, Achterberg EP, Rost B (2016) Interactive effects of ocean acidification and nitrogen limitation on two bloom-forming dinoflagellate species. Mar Ecol Prog Ser 543:127–140

Falkowski PG, Raven AR (2007) Aquatic photosynthesis, 2nd edn. Princeton University Press, Princeton, NJ

Falkowski PG, Katz ME, Knoll AH, Quigg A, Raven JA, Schofield O, Taylor FJ (2004) The evolution of modern eukaryotic phytoplankton. Science 305:354–360

Feely RA, Doney SC, Cooley SR (2009) Ocean acidification: present conditions and future changes in a high-CO_2 world. Oceanography 22:36–47

Giordano M, Beardall J, Raven JA (2005) CO_2 concentrating mechanisms in algae: mechanisms, environmental modulation, and evolution. Annu Rev Plant Biol 56:99–131

Granum E, Roberts K, Raven JA, Leegood RC (2009) Primary carbon and nitrogen metabolic gene expression in the diatom *Thalassiosira pseudonana* (Bacillariophyceae): diel periodicity and effects of inorganic carbon and nitrogen. J Phycol 45:1083–1092

Gunderson AR, Armstrong EJ, Stillman JH (2016) Multiple stressors in a changing world: the need for an improved perspective on physiological responses to the dynamic marine environment. Annu Rev Mar Sci 8:357–378

Halsey KH, Jones BM (2015) Phytoplankton strategies for photosynthetic energy allocation. Annu Rev Mar Sci 7: 265–297

Hennon GMM, Quay P, Morales RL, Swanson LM, Armbrust EV (2014) Acclimation conditions modify physiological response of the diatom *Thalassiosira pseudonana* to elevated CO_2 concentrations in a nitrate-limited chemostat. J Phycol 50:243–253

Hennon GMM, Ashworth J, Groussman RD, Berthiaume C and others (2015) Diatom acclimation to elevated CO_2 via cAMP signaling and coordinated gene expression. Nat Clim Change 5:761–765

Hopkinson BM, Dupont CL, Allen AE, Morel FMM (2011) Efficiency of the CO_2-concentrating mechanism of diatoms. Proc Natl Acad Sci USA 108:3830–3837

Li W, Gao K, Beardall J (2012) Interactive effects of ocean acidification and nitrogen-limitation on the diatom *Phaeodactylum tricornutum*. PLOS ONE 7:e51590

Li G, Brown CM, Jeans JA, Donaher NA, McCarthy A, Douglas A (2015) The nitrogen costs of photosynthesis in a diatom under current and future pCO_2. New Phytol 205: 533–543

Lomas MW (2004) Nitrate reductase and urease enzyme activity in the marine diatom *Thalassiosira weissflogii* (Bacillariophyceae): interactions among nitrogen substrates. Mar Biol 144:37–44

Losh JL, Morel FMM, Hopkinson BM (2012) Modest increase in the C:N ratio of N-limited phytoplankton in the California Current in response to high CO_2. Mar Ecol Prog Ser 468:31–42

Losh JL, Young JN, Morel FMM (2013) Rubisco is a small fraction of total protein in marine phytoplankton. New Phytol 198:52–58

McGinn PJ, Morel FMM (2008) Expression and regulation of carbonic anhydrases in the marine diatom *Thalassiosira pseudonana* and in natural phytoplankton assemblages from Great Bay, New Jersey. Physiol Plant 133:78–91

Mehrbach C, Culberso CH, Hawley JE, Pytkowic RM (1973) Measurement of apparent dissociation constants of carbonic acid in seawater at atmospheric pressure. Limnol Oceanogr 18:897–907

Moore CM, Mills MM, Arrigo KR, Berman-Frank I and others (2013) Processes and patterns of oceanic nutrient limitation. Nat Geosci 6:701–710

Orr JC, Fabry VJ, Aumont O, Bopp L and others (2005) Anthropogenic ocean acidification over the twenty-first century and its impact on calcifying organisms. Nature 437:681–686

Parker MS, Armbrust EV (2005) Synergistic effects of light, temperature, and nitrogen source on transcription of genes for carbon and nitrogen metabolism in the centric diatom *Thalassiosira pseudonana* (Bacillariophyceae). J Phycol 41:1142–1153

Pierrot D, Lewis E, Wallace D (2006) MS Excel program developed for CO_2 system calculations. Carbon Dioxide Information Analysis Center, US Department of Energy, Oak Ridge National Laboratory, Oak Ridge, TN

Poulsen N, Kroger N (2005) A new molecular tool for transgenic diatoms: control of mRNA and protein biosynthesis by an inducible promoter–terminator cassette. FEBS J 272:3413–3423

Raven JA, Kubler JE, Beardall J (2000) Put out the light, and then put out the light. J Mar Biol Assoc UK 80:1–25

Reinfelder JR (2011) Carbon concentrating mechanisms in eukaryotic marine phytoplankton. Annu Rev Mar Sci 3: 291–315

Reinfelder JR (2012) Carbon dioxide regulation of nitrogen and phosphorus in four species of marine phytoplankton. Mar Ecol Prog Ser 466:57–67

Riebesell U, Schulz K, Bellerby RGJ, Botros M and others (2007) Enhanced biological carbon consumption in a high CO_2 ocean. Nature 450:545–548

Roberts SB, Lane TW, Morel FMM (1997) Carbonic anhydrase in the marine diatom *Thalassiosira weissflogii* (Bacillariophyceae). J Phycol 33:845–850

Roberts K, Granum E, Leegood RC, Raven JA (2007) C_3 and C_4 pathways of photosynthetic carbon assimilation in marine diatoms are under genetic, not environmental control. Plant Physiol 145:230–235

Rost B, Zondervan I, Wolf-Gladrow D (2008) Sensitivity of phytoplankton to future changes in ocean carbonate

chemistry: current knowledge, contradictions and research directions. Mar Ecol Prog Ser 373:227–237

Rouco M, Branson O, Lebrato M, Iglesias-Rodriguez MD (2013) The effect of nitrate and phosphate availability on *Emiliania huxleyi* (NZEH) physiology under different CO_2 scenarios. Front Microbiol 4:155

Sabine CL, Feely RA (2007) The oceanic sink for carbon dioxide. In: Reay D, Hewitt N, Grace J, Smith K (eds) Greenhouse gas sinks. CABI Publishing, Wallingford, p 31–49.

Sabine CL, Feely RA, Gruber N, Key RM and others (2004) The oceanic sink for anthropogenic CO_2. Science 305: 367–371

Satoh D, Hiraoka Y, Colman B, Matsuda Y (2001) Physiological and molecular biological characterization of intracellular carbonic anhydrase from the marine diatom *Phaeodactylum tricornutum*. Plant Physiol 126:1459–1470

Shi D, Li W, Hopkinson BM, Hong H, Li D, Kao SJ, Lin W (2015) Interactive effects of light, nitrogen source, and carbon dioxide on energy metabolism in the diatom *Thalassiosira pseudonana*. Limnol Oceanogr 60:1805–1822

Sunda WG, Price NM, Morel FMM (2005) Trace metal ion buffers and their use in culture studies. In: Andersen RA (ed) Algal culturing techniques. Elsevier Academic Press, New York, NY, p 35–63

Taucher J, Jones J, James A, Brzezinski MA, Carlson CA, Riebesell U, Passow U (2015) Combined effects of CO_2 and temperature on carbon uptake and partitioning by the marine diatoms *Thalassiosira weissflogii* and *Dactyliosolen fragilissimus*. Limnol Oceanogr 60:901–919

Tortell PD, Payne CD, Li Y, Trimborn S and others (2008) CO_2 sensitivity of Southern Ocean phytoplankton. Geophys Res Lett 35:L04605

Vergara JJ, Berges JA, Falkowski PG (1998) Diel periodicity of nitrate reductase activity and protein levels in the marine *Thalassiosira pseudonana* (Bacillariophyceae). J Phycol 34:952–961

Wu Y, Gao K, Riebesell U (2010) CO_2-induced seawater acidification affects physiological performance of the marine diatom *Phaeodactylum tricornutum*. Biogeosciences 7:2915–2923

Wu H, Cockshutt AM, McCarthy A, Campbell DA (2011) Distinctive photosystem II photoinactivation and protein dynamics in marine diatoms. Plant Physiol 156:2184–2195

Yang G, Gao K (2012) Physiological responses of the marine diatom *Thalassiosira pseudonana* to increased pCO_2 and seawater acidity. Mar Environ Res 79:142–151

Zhang H, Byrne RH (1996) Spectrophotometric pH measurements of surface seawater at in-situ conditions: absorbance and protonation behavior of thymol blue. Mar Chem 52:17–25

Appendix 1

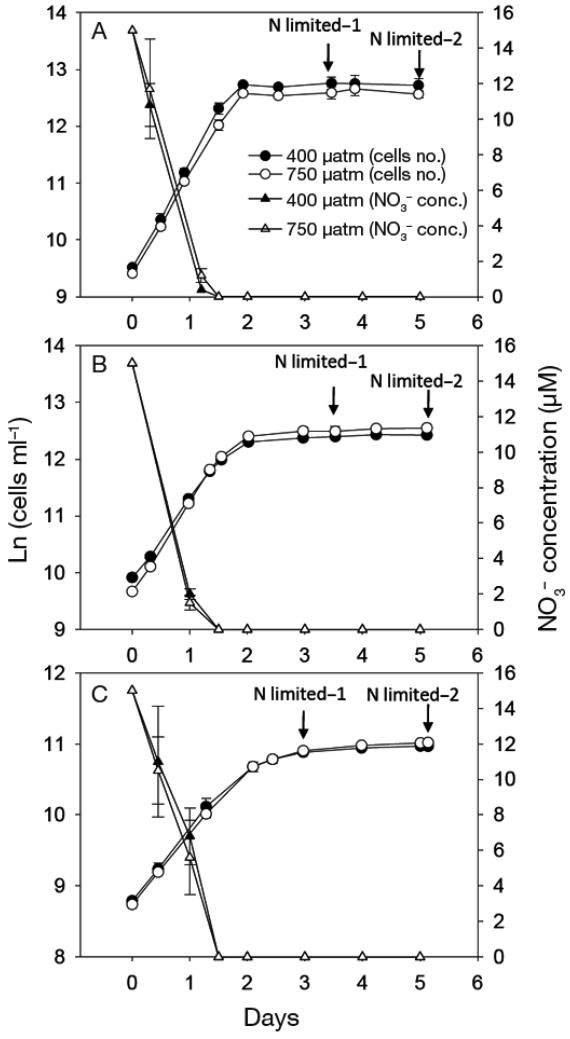

Fig. A1. The growth curve (left *y*-axis) and NO_3^- concentrations (right *y*-axis) in the culture media of (A) *Thalassiosira pseudonana*, (B) *Phaeodactylum tricornutum*, and (C) *T. weissflogii* acclimated to 2 different pCO_2 levels (400 and 750 µatm). The cells were grown in Aquil* media and NO_3^- was added to the initial concentration of 15 µM. Arrows signify the time points when the 2 N-limited treatments were sampled. N-limited-1 and N-limited-2 represent cultures harvested at 36 and 72 h after entering the stationary phase, respectively

Editorial responsibility: Morten Pedersen, Roskilde, Denmark

Submitted: September 12, 2016 Accepted: December 22, 2016
Proofs received from author(s): February 25, 2017